

High Frequency Viscoelasticity of Carbon Black Filled Compounds

M. Gerspacher*, C. P. O'Farrell, L. Nikiel, H. H. Yang

Sid Richardson Carbon Company
Fort Worth Research Center
4825 North Freeway
Fort Worth, TX 76106

and

F. Le Méhauté

Institut Supérieur des Matériaux du Mans
44, Avenue F. A. Bartholdi
72000 Le Mans
France

Presented at the 149th Spring Technical Meeting
Rubber Division, American Chemical Society
Montreal, Canada
May 5-8, 1996

* Speaker

Abstract:

A high frequency viscoelasticity spectrometer, using the state-of-the-art ultrasonic technology, was constructed. The longitudinal and shear waves characteristics were measured in rubber compounds to obtain the attenuation coefficient, α , and sound velocity, ν . Preliminary results were obtained for a number of filled and unfilled polymers. The grade of carbon black used, filler loading, crosslinking density and filler dispersion were varied during the study. Temperature sweep from -100°C to $+60^{\circ}\text{C}$ were also studied. It was found that the polymer type had a greater influence on α and ν than did the grade of carbon black, loading or dispersion. The experimental data show that shear waves do not propagate in the rubbery state. Above the glass transition temperature, T_g , the longitudinal wave measurements could be sufficient to determine the high frequency dynamic properties of filled and unfilled polymers to characterize a tire tread compound. The temperature sweep measurements allowed the determination of the T_g of polymers at high frequency. It is proposed that the described method of measuring α and ν be used as a laboratory tool for potential tire traction prediction.

I. Introduction

Reinforcing properties of carbon black are very well documented in the literature [1-9], however, the effects of carbon black on specific tire properties are not always fully predicted by existing tire material characterizations (i.e. tire traction). The existing approaches to characterize traction properties of tread compounds, (i.e. $\tan \delta$ at 0°C), may be able to differentiate between polymers but do not predict the carbon black influence on tire traction behavior. One current method of testing tire traction (i.e. the "peak and slide GM traction test") suggests that high frequency viscoelastic properties of rubber tread compounds can be used to predict traction behavior. It can be shown that when a trailer tire is locked, at 60 mph, the deformation of the rubber at the tread-road interface occurs in the MHz frequency range. The following sections of this paper will summarize the theoretical and experimental approach used by SRCC to build and evaluate a high frequency viscoelastic spectrometer.

II. Experimental Set-up.

The SRCC high frequency viscoelastic tester consists of three major components (i.e. pulser/receiver, measuring cell and oscilloscope) as shown in Fig. 1. The ultrasonic pulser/receiver, model 5055PR (Panametrics, Inc.) capable of generating a wide frequency band from 0.1 to 10 MHz, is the main component. The immersion measurement cell is equipped with two ultrasonic transducers. One piezoelectric transducer is used as a transmitter which generates ultrasonic waves. When high frequency electrical current from the pulser/receiver is applied to the piezoelectric crystal it vibrates according to a characteristic frequency. These mechanical vibrations are in turn detected by the second transducer which functions as a receiver. In the receiver the

mechanical vibrations are converted to an electric current, the magnitude of which is proportional to the sound pressure. The immersion transducers have a frequency centered around 1 MHz.

Ethyl alcohol is used as a required coupling agent inside the spectrometer [10]. The low freezing point of ethanol provides a media to cover a wide range of temperatures. Ethanol also wets the rubber surface which maximizes the ultrasonic wave propagation. During the course of the study no sample swelling or material deterioration in the coupling liquid was observed.

The sample holder (see Fig. 3) can rotate around an axis normal to the two transducers line. Its angle of rotation is monitored with high accuracy by using a rotary stage, like those commonly used in optical components. All signals are monitored on a digital signal processing capabilities oscilloscope (Tektronix Corp., model # TDS 524A). The temperature of the measuring cell is stabilized using a Lauda RM6 circulating bath for temperatures above 0°C. An in-house designed gas/liquid nitrogen cooling system allows experimental temperatures to range between -100°C and 0°C. The temperature is monitored by a thermocouple placed close to the rubber sample and is controlled by an Omega CN3201 process controller. The temperature stabilization is within $\pm 0.2^\circ\text{C}$.

Rubber samples were mixed using an internal mixer (Haake Rheocord 90) according to the D3191 ASTM standard recipe. The curing mold produced cylindrical samples featuring highly parallel, mirror-like finished surfaces. The samples were cured at 160°C using constant crosslinking density (t'90 + mold lag). About 25 samples of different thicknesses were prepared for a given formulation. Sample thickness ranged from 1 to 20 mm. Seven different polymers (Natural Rubber, Natsyn 2200, SBR 1500, Sn-SSBR, Duradene 706, Duradene 709 and Duradene 711), and thirteen grades of carbon black were used in the initial study.

III. Theoretical Considerations.

A. Homogeneous Material.

Different types of ultrasonic waves propagate in solids depending on how the direction of wave propagation is related to the direction of vibration, and also on the boundary conditions. The most common types of mechanical waves in a solids are:

- 1) Longitudinal waves where the direction of vibration is parallel to the direction of propagation.
- 2) Shear (or transverse) waves where the vibration is perpendicular to the wave propagation.

Usually, the longitudinal waves propagate about twice as fast as the shear wave. The amplitudes of the longitudinal and the shear waves decay as δ^{-1} , δ being the distance from the interface, in the region away from the surface. Close to the surface the decay is faster, as δ^{-2} [10-12]. The possibility of interference of the original pulse with the reflected signal requires additional attention when planning experiments. It can be shown [10-12], that samples with thicknesses larger than the wave length should be used in order to avoid these interferences.

The ultrasonic method of inducing high frequency deformation is generally limited to very low strain deformation. The SRCC's experimental settings generate amplitude of deformation between 10^{-8} to 10^{-9} m [10].

Lets consider the transmission of ultrasonic waves inside a homogeneous material and the reflection of these waves encountering a second homogeneous media (Fig. 2). In the range of temperatures used the attenuation of the coupling liquid is neglectible. The ultrasound signal with sound pressure p_0 is emitted from the first transducer. At the first interface (liquid - rubber sample) a portion of the signal, p_r , is reflected. The reflection

coefficient R_I is defined as [10]:

$$R_1 = \frac{Z_1 - Z_2}{Z_1 + Z_2} \quad (1)$$

where Z_i is the acoustic impedance of the i medium defined as: $Z_i = \rho_i v_i$. In this paper index 1 refers to the coupling liquid and 2 to the rubber compound.

The signal p_2 (see Fig. 2) is then given by:

$$p_2 = p_0(1 - R_1) \quad (2)$$

The pressure p_3 of the ultrasonic signal at the second interface can be expressed according to the Beer's law of absorption:

$$p_3 = p_2 \exp(-\alpha d) \quad (3)$$

where α is the attenuation coefficient and d is the sample thickness. Finally, after the reflection at the second interface according to equation 1 the intensity detected by the second transducer can be represented by the following equation:

$$p = p_0(1 - R^2)\exp(-\alpha d) \quad (4)$$

The attenuation coefficient α is calculated by fitting equation 4 to the experimental data.

A.1. Longitudinal Wave.

The velocity of the longitudinal sound wave in the rubber samples is calculated using the following formula:

$$v_L = \frac{d}{(t - t_0) + \frac{d}{v_A}} \quad (5)$$

where d is the sample thickness, t_0 is the propagation time obtained without sample, t is the time with the sample present and v_A is the speed of sound in the coupling liquid at a given temperature.

A.2. Shear Wave.

The measurements of the shear wave velocity can be accomplished by using the rotating plate method [13] (see Fig. 3) or the modified rotating plate method [14]. When the surface of the sample is perpendicular to the direction of propagation of the longitudinal wave, only the longitudinal wave is propagated through the sample. However, when the incident angle is different from the normal (90°) the two types of waves, the longitudinal wave and the shear wave, appear in the sample. By further rotating the sample to the specific angle determined by the Snell law [10,13], the longitudinal wave amplitude vanishes and only the shear wave is propagated. When the shear wave is escaping from the sample it is converted back to longitudinal wave and can be detected by the receiving ultrasonic transducer. The final equation for calculating the shear wave velocity can be written as [13]:

$$v_T = \frac{A}{\left(t - \left(t_0 - \frac{C}{v_A} \right) \right)} \quad (6)$$

where

$$A = \frac{D}{\sqrt{1 - (B \sin \psi)^2}},$$

$$B = \left[\left(\cos \psi - \frac{v_A(t_0 - t)}{D} \right)^2 + \sin^2 \psi \right]^{\frac{1}{2}},$$

$$C = A \cos(\varphi - \psi),$$

and

$$\varphi = \cos^{-1}\left(\frac{D}{A}\right).$$

The meaning of the angles φ and ψ is presented in Fig. 3.

A.3. Dynamic Modulus.

In a *homogeneous* medium, by solving the wave equation [15], one can calculate the longitudinal storage (Eq. 7) and the longitudinal loss modulus (Eq. 8) as well as the shear storage (Eq. 9) and the shear loss modulus (Eq. 10).

$$M' = \frac{\rho v_L^2 (1 - r_L^2)}{(1 + r_L^2)^2} \quad (7)$$

$$M'' = \frac{2\rho r_L v_L^2}{(1 + r_L^2)^2} \quad (8)$$

$$G' = \frac{\rho v_T^2 (1 - r_T^2)}{(1 + r_T^2)^2} \quad (9)$$

$$G'' = \frac{2\rho r_T v_T^2}{(1+r_T^2)^2} \quad (10)$$

where ρ is the sample density, $r_L = (\alpha_L \lambda_L) / 2\pi$ and $r_T = (\alpha_T \lambda_T) / 2\pi$. The symbols $\alpha_L, \alpha_T, \lambda_L$ and λ_T denotes the attenuation coefficients and the wavelength for the longitudinal and the shear wave respectively

The bulk modulus, $K^* = K' + iK''$, can be obtained from the following equation [1]:

$$K^* = M^* - 4/3G^* \quad (11)$$

where $M^* = M' + iM''$ and $G^* = G' + iG''$.

In the present study we will concentrate on the longitudinal wave propagation, since it will be shown as mentioned elsewhere [10-12], that in a "liquid"/rubbery plateau the shear wave does not propagate.

B. Heterogeneous Material.

On a microscopic scale a carbon black filled rubber compound is not a homogeneous material. The carbon black network interpenetrates the polymer network forming a two phase system. However, within a larger heterogenous sample, individual homogeneous domain can be isolated. The scattering and transmission phenomena at an interface are identical, whether the interface is for a truly homogeneous sample or is an isolated homogeneous fragment within a larger heterogeneous mixture. Because the number of interfaces can be very large in the latter case, the overall interpretation of the obtained results is much more complicated. In particular the following considerations

have to be accounted for: the scattering at the interface, the difference in the speed of sound, and the attenuation coefficient in the carbon black and polymer phase. Depending on the degree of the filler dispersion and the filler loading, a certain extent of carbon black - polymer interface is created. At such an interface a part of the ultrasound wave is reflected in different directions. The overall amount of these reflections depends on the value of the reflection coefficient as well as the extent of interfaces in the volume of sample exposed to the ultrasonic vibrations. Due to the very small dimension of the individual phase of the heterogeneous composite, the reflected portion of the signal from multiple reflections can significantly interfere with the original signal, changing the information which it carries. Taking into account all possible mechanisms one can realize that this is a very complicated phenomena which requires a new theoretical approach to correctly calculate the attenuation coefficient and the respective viscoelastic properties. One approach [16], based on a simplified heterogeneous model (Fig. 4) involves a rubber sample that is divided in n number of layers with infinitesimally small thicknesses. The surface of the carbon black and the polymer phase in each layer is constant throughout the sample and described as S_{CB} and S_P . By generalizing the reflection and the transmission concepts presented above, one can obtain the following equation describing the intensity of the transmitted signal:

$$p = p_0 \left(R_1 \frac{S_{CB}}{S_{CB} + S_P} + R_2 \frac{S_P}{S_{CB} + S_P} \right) e^{-d \left(\alpha_{CB} \frac{S_{CB}}{S_{CB} + S_P} + \alpha_P \frac{S_P}{S_{CB} + S_P} \right)} \quad (12)$$

where R_1 is the reflection coefficient at the rubber-carbon black interface, R_2 is the reflection coefficient at the carbon black-rubber interface, α_{CB} is the attenuation coefficient of the carbon black phase, α_P is the attenuation coefficient of the polymer phase and d is the sample thickness. Symbols p_0 and p represent the incident and

transmitted sound pressure, respectively.

The attenuation coefficient of a heterogeneous material has additive properties as expressed in Eq. 12. By measuring the attenuation coefficient separately for an individual phase one should be able to estimate the attenuation coefficient for a bulk heterogeneous sample. It will be shown later, in this paper, that by using this model it is possible to qualitatively predict the dependency of the results on the filler dispersion.

IV. Results.

In order to evaluate the high frequency spectrometer as a tool for predicting tire traction, the following experiments were performed: the influence of polymer type, carbon black loading, carbon black grade, filler dispersion and crosslinking density on the attenuation and sound velocity of the ultrasound wave. Additionally, these studies were performed over a wide range of temperatures.

Three characteristics ,(i.e. the compound density, the sound velocity, and the attenuation coefficient) are measured for each formulation. The density of the cured compound was determined at room temperature (25°C). The sample is then placed in the spectrometer with its surface set normal to the direction of the sound propagation. After stabilization of the temperature, measurements were taken using the digital oscilloscope. Both the incident and the transmitted amplitude, as well as the wave propagation time were evaluated in each sample. In order to evaluate both the sound attenuation and the sound velocity for each case, the experiment was repeated using 25 samples of different thicknesses prepared according to the same formulation.

A. Polymer Study.

The polymer T_g (glass transition temperature) is an essential characteristic of a polymer, however, this T_g is frequency dependent [1]. In Table I, the Differential Scanning Calorimetry (DSC) measured thermal glass transition temperature, T_g^0 , is presented for the compounds tested (i.e. SBR-1500, Duradene 706, Duradene 709, Duradene 711, Natural Rubber and Sn-SSBR). The high frequency experiments were performed at room temperature. In general, as can be seen in Fig. 5, the lower the thermal glass transition temperature, T_g^0 , the lower the attenuation coefficient, α_L , obtained for the longitudinal wave propagation.

The longitudinal wave velocity values, v_L , are presented in Fig. 6. As can be seen from this figure, the speed of sound in the unfilled rubber compounds studied lies between 1550 and 1620 m/s, at the given experimental conditions, and is dependent on the glass transition temperature, T_g^0 . Lower values of the sound velocity are observed for the polymers with low glass transition temperature.

As it is shown below, the presence of carbon black in the polymer affects both α_L and v_L . The attenuation coefficient α_L is always higher for carbon black filled compounds. Carbon black filled compounds are shown to also have higher values of v_L than their unfilled counterparts for all polymers studied.

B. Loading Study.

Detailed loading studies were limited to one polymer and three grades of carbon black. All data were obtained at room temperature (25°C) for carbon black loadings ranging from 0 phr up to 80 phr. Tin coupled solution SBR (Sn-SSBR) was used because of its relatively high T_g^0 and the greater potential for the shear wave investigation. The

shear wave phenomena will be addressed later in this paper. Carbon blacks used in this study were trade grades N110, N330 and SRCC's experimental high structure, 'three-dimensional' black, XLH81. XLH81 is proven to be easier to disperse than the conventional grades of carbon black. As can be seen from Fig. 7 the attenuation coefficient α_L increases with the carbon black loading for each grade studied. The data are indistinguishable up to about 40 phr of carbon black loading, however, it is evident that at higher loading the XLH81 has a higher attenuation coefficient, α_L , than N110 and N330. The higher attenuation coefficient, α_L , obtained for the XLH81 black suggests that the dispersion of carbon black may be responsible for the sound attenuation phenomena.

The longitudinal wave velocity measurements presented in Fig. 8 show lower values for the XLH81 compared to the conventional grades.

C. Different Grades of Carbon Black.

The objective of these experiments was to evaluate the influence of the filler type on the high frequency properties of cured compounds. Thirteen grades of SRCC carbon black, at 50 phr loading level, were evaluated in a D3191 type formulation. Similar to the previous study, Sn-SSBR was used. The attenuation coefficient α_L is plotted versus BET “nitrogen number”, N_2SA , in Fig. 9. A decreasing trend of α_L and an increasing trend of ν_L are observed for increasing values of N_2SA . The reason for these trends is not well understood for the time being. The difference in aggregate size and/or ease dispersion may explain these phenomenon. More studies are underway to clarify this point.

D. Filler Dispersion Study.

In order to verify the filler dispersion hypothesis, the attenuation coefficient α_L and the longitudinal wave velocity v_L were measured for samples mixed for 1, 2, 4, 6 and 10 minutes using the Haake internal mixer. The polymers chosen for this study were SBR-1500 and Sn-SSBR. The filler used was the ultra-high structure experimental carbon black, XLH142 at 50 phr loading. The dispersion of carbon black was verified by the Mechanical Scanning Microscope (MSM) equipped with the 2 μm stylus. The parameter characterizing filler dispersion using the MSM technique, is known as the micro-roughness factor, R_a . In general, higher values of R_a for a given set of samples indicate poorer filler dispersion. The dependence of filler dispersion on the mixing time can clearly be seen by examining the data in Fig. 11. The shorter the SBR 1500 mixing time the poorer the carbon black dispersion. Also, the relationship between the filler dispersion and the attenuation coefficient is obvious from Fig. 12. As expected, the attenuation coefficient α_L is higher for better dispersed samples. Eq. 12 was applied for qualitative evaluation of the experimental data. When the filler dispersion is better, S_{CB} increases and consequently the attenuation coefficient increases. However, the mechanism of carbon black dispersion is a very complicated phenomena. and more studies are necessary to correlate carbon black dispersion and the ultrasound energy dissipation. In particular, the attenuation coefficient α_L of carbon black itself has to be evaluated in order to apply quantitatively Equation 12.

E. Crosslinking Density.

These experiments were performed in order to evaluate the effects of crosslinking density of rubber vulcanizates on the ultrasound wave propagation. Both the amount of

curatives and the curing time were varied during the course of the experiment. These studies were performed for both filled and unfilled polymers. No significant differences in the attenuation coefficient α_L were observed for the carbon black filled compounds using sulfur in the range of 50 to 200 % of the nominal value. In this case α_L changes only by 0.5 %. However the changes were significant for the unfilled compounds where the coefficient α_L increased about 10 % when the amount of sulfur was increased from 50 to 200 % of the nominal value.

When the curing time was varied, more significant changes in the value of the α_L were observed. The attenuation coefficient was significantly lower for under-cured samples and reaches a plateau for t'90 and longer curing times. From Fig. 13 one can conclude that over-curing has little or no effect on the attenuation coefficient α_L .

F. Temperature Study.

Since the glass transition temperature T_g may govern the important dynamic properties of polymers, systematic studies of the high frequency viscoelasticity in a wide range of temperatures were performed. It is well known that T_g measured by different methods gives different values. The Differential Scanning Calorimetry (DSC) values of T_g^0 are usually lower than other methods. The DSC value depends strongly on the rate of heating, and the T_g values obtained are referred to as a thermal glass transition temperature [17]. Other methods such as Nuclear Magnetic Resonance (NMR) and Dynamic Mechanical Analysis (DMA) give higher values of glass transition temperature and these values are referred to as dynamic glass transition temperatures. The WLF equation (Williams, Landel, Ferry) [1] predicts that the T_g of many polymers changes by 6 to 7 degrees per decade of frequency change. It was expected that the information obtained from the ultrasound experiments conducted at 1 MHz frequency would also

contribute to the understanding of the glass transition phenomena. Indeed, the results obtained for the unfilled Sn-SSBR, as well as for the carbon black filled compound, indicate a shift of the T_g toward higher temperatures (see Fig. 14). In this case the position of the maximum of the attenuation coefficient α_L was assumed to be the glass transition temperature. We have observed a shift of about 50 degrees between the DSC glass transition temperature and the value obtained from the high frequency viscoelasticity experiment at 10^6 Hz.

The values of the attenuation coefficient α_L for the unfilled polymer coincide with the values obtained for the filled compounds only in the glassy zone. Above the T_g the ultrasound energy of the unfilled compounds is dissipated at a faster rate than for the filled compound.

G. Shear Wave Evaluation.

There is existing evidence in the literature that shear waves do not propagate in the liquid phase [10-12]. Since a rubber compound above its glass transition temperature can be considered as a liquid state, the shear wave propagation was studied in the carbon black filled compound. The rotating plate method was used to evaluate shear waves in the sample [13]. A polymer with relatively high T_g^0 , i.e. Sn-SSBR, was used in these experiments. As can be seen from Fig. 15, the amplitude of the shear wave vanishes to an undetectable level about 25 degree below the T_g measured at 1 MHz. The attenuation coefficient data are presented in Fig. 16. Since the most important dynamic tire compound properties are tested in the rubbery plateau even at 1 MHz around room temperature it is of little usefulness from an application point of view, to investigate the shear wave that occurs only in the glassy state.

H. Attenuation Coefficient α_L of Carbon Black.

In order to evaluate the attenuation coefficient α_L of carbon black itself a special technique was applied. A measuring cell with a variable distance between the immersion transducers was constructed. Carbon black in the form of paste made with ethyl alcohol was used. The concentration of carbon black ranged from about 10% to about 25% by weight. Lower concentrations of carbon black do not provide well dispersed homogeneous samples while samples with higher concentrations of carbon black did contain trapped air inside the filler structure. Measurements obtained for loose N234 and presented in Fig. 17, suggest that at room temperature the attenuation coefficient α_L can be higher for carbon black than most polymers. To verify this finding, the measurements of highly isotropic graphite with randomly distributed crystallographic planes and very small L_a , were performed. The attenuation coefficient α_L obtained in this study was about 0.09 [1/mm] which indicate that carbon black indeed may have a relatively high attenuation coefficient. However, more systematic investigation is necessary to verify and confirm these results. Such measurements are in progress at SRCC and will be presented in the next publication.

IV. WLF Equation.

In order to compare the high frequency viscoelasticity measurements with the low frequency/low strain experiment, temperature and frequency sweeps were performed using a Rheometrics System IV Mechanical Spectrometer. All data were reduced to mastercurves following the universal WLF relationship [1]. On the basis of the assumption that all relaxation mechanisms in a non-filler loaded specimen have the same

temperature dependence, it is possible to reduce all the data to the same reference temperature T_0 by shifting the $\log(G', G'' \text{ or } \tan \delta)$ vs $\log(\text{frequency})$ curves along the frequency axis. However, this assumption is invalid for the carbon black loaded polymers since the carbon black network dominates the dynamic properties of the compound. Only at temperatures close to the glass transition temperature does the polymer network gain the leading role. This results are presented in Fig. 18. When the values of G' are extrapolated to the frequency of 1 MHz using the WLF equation, the carbon black filled compounds gain a significantly lower value of G' compared to the unfilled compound as presented in Fig. 19. The data obtained from the high frequency viscoelasticity experiments suggest that the attenuation coefficient representing the rate of energy dissipation is higher for the filled compounds (see Fig 20). Due to these facts an application of the WLF equation for the carbon black filled compounds is questionable. An alternative method such as the ultrasound measurement should be applied to obtain the high frequency dynamic properties of filled polymers.

VI. Summary and Conclusions.

During the course of this study, the high frequency ultrasound method of evaluating the dynamic properties of filled and unfilled polymers was proven to be very promising. It is possible by using this method to observe the influence of different compound parameters, i.e. polymer and filler type, filler loading, mixing and curing conditions, on the high frequency dynamic properties. In this paper the attenuation coefficients and the longitudinal wave velocities obtained for various compounds under a wide range of experimental conditions were presented. Since the calculations of dynamic modulus for the heterogeneous materials represent a very complicated theoretical problem these issues will be addressed in later publications.

Polymer type has the greatest influence on the attenuation coefficient value as well as on the longitudinal wave velocity. The filler seems to play a secondary role. All performed experiments suggests that carbon black dispersion has a large influence on the obtained results, suggesting that better filler dispersion allows better energy dissipation.

The experimental method presented in this paper may also be valuable in obtaining the glass transition temperature in the frequency range from 0.5 MHz to 10 MHz, depending on the transducers used.

The data obtained for the shear wave measurements indicate that in rubbery state the shear wave does not propagate. This result can lead to the conclusion that the longitudinal wave measurements can be sufficient in predicting high frequency dynamic properties of rubber.

It would be of great interest to compare tire traction data with high frequency tread compound behavior. These data will be reported as soon as available.

Acknowledgments

The authors would like to acknowledge Sid Richardson Carbon Company management for their support and authorization to publish this paper. We also thank Prof. T. W. Zerda (TCU) and Dr. A. Le Méhauté (ISMANS) for useful discussions.

References

- [1]. J. D. Ferry, “*Viscoelastic Properties of Polymers*”, J. Wiley & Sons, New York, 1980.
- [2]. A. I. Medalia, *Rubber Chem. Technol.* **51** (1978) 437.
- [3]. M. Gerspacher, C. P. O’Farrell, and H. H. Yang, *Elastomerics*, **11** (1990) 23.
- [4]. G. Kraus, *Adv. Polymer Sci.* **8** (1971) 155.
- [5]. G. Kraus, “*Reinforcement of Elastomers*”, Wiley-Interscience, New York, 1965.
- [6]. A. Voet, *Macromol. Rev.* **15** (1980) 327.
- [7]. E. M. Dannenberg, *Rubber Chem. Technol.* **48** (1975) 410.
- [8]. J. B. Donnet and A. Voet, “*Carbon Black, Physics, Chemistry, and Elastomer Reinforcement*” MerceL Dekker, Inc., New York, 1976.
- [9]. J. B. Donnet, R. C. Bansal, and M. J. Wang, “*Carbon Black, Science and Technology*”, MerceL Dekker, Inc., New York, 1993
- [10]. J. Krautkrämer and H. Krautkrämer, “*Ultrasonic Testing of Materials*”, Springer-Verlag, New York, 1990.
- [11]. T. F. Hueter and R. H. Bolt, “*Sonics, Techniques for the Use of Sound and ultrasound in Engineering and Science*”, J. Wiley & Sons, Inc., New York, 1966.
- [12]. J. R. Frederick, “*Ultrasonic Engineering*”, J. Wiley & Sons, New York, 1965.
- [13]. Y. Wada, H. Hirose, T. Asano, and S. Fukutomi, *J. Phys. Soc. Japan*, **14** (1959) 1064.
- [14]. R. Kono, *J. Phys. Soc. Japan*, **15** (1960) 718.
- [15]. M. A. Meyers, “*Dynamic Behavior of Materials*”, J. Wiley & Sons, Inc., New York, 1994.

[16]. C. Tricot, *private communication*.

[17]. G. Heinrich, N. Rennar, and H. Dumler, *Kautsch. Gummi Kunstst.* **49** (1996) 32.

Table. I The Differential Scanning Calorimetry (DSC) values of the glass transition temperature, T_g , obtained for polymers studied.

Polymer	Sn-SSBR	SBR 1500	Duradene 709	Natural Rubber	Duradene 706	Duradene 711
T_g [°C]	-26	-43	-47	-56	-57	-67

Figure Captions

- Fig. 1 Schematic diagram of SRCC's apparatus for measuring high frequency viscoelasticity using ultrasonic method.
- Fig. 2 Schematic representation of reflection, transmission and signal attenuation phenomena at the interface of two media.
- Fig. 3 Rotating plate method of obtaining the shear wave propagation.
- Fig. 4 Prof. Tricot's model of carbon black filled polymer as a heterogeneous material.
- Fig. 5 Attenuation coefficient, α_L , plotted versus DSC glass transition temperature obtained for carbon black (50 phr XLH81) filled polymers (Natural Rubber ($T_g = -56^\circ\text{C}$), SBR 1500 ($T_g = -43^\circ\text{C}$), Sn-SSBR ($T_g = -26^\circ\text{C}$), Duradene 706 ($T_g = -57^\circ\text{C}$), Duradene 709 ($T_g = -47^\circ\text{C}$) and Duradene 711 ($T_g = -67^\circ\text{C}$)).
- Fig. 6 Longitudinal wave velocity, v_L , plotted versus DSC glass transition temperature obtained for carbon black (50 phr XLH81) filled polymers (Natural Rubber ($T_g = -56^\circ\text{C}$), SBR 1500 ($T_g = -43^\circ\text{C}$), Sn-SSBR ($T_g = -26^\circ\text{C}$), Duradene 706 ($T_g = -57^\circ\text{C}$), Duradene 709 ($T_g = -47^\circ\text{C}$) and Duradene 711 ($T_g = -67^\circ\text{C}$)).

Fig. 7 Attenuation coefficient, α_L , as a function of carbon black loading. Sn-SSBR used as the polymer.

Fig. 8 Longitudinal wave velocity, v_L , as a function of carbon black loading. Sn-SSBR used as the polymer.

Fig. 9 Attenuation coefficient, α_L , obtained for different grades of carbon black at 50 phr loading in Sn-SSBR, plotted against nitrogen specific surface area, N_2SA .

Fig. 10 Longitudinal wave velocity, v_L , obtained for different grades of carbon black at 50 phr loading in Sn-SSBR, plotted against nitrogen specific surface area, N_2SA .

Fig. 11 Micro-roughness parameter, R_a , obtained for SBR 1500 loaded with 50 phr XLH142 (circles) and Sn-SSBR 1500 loaded with 50 phr XLH142 (squares), as a function of mixing time.

Fig. 12 Relationship between the attenuation coefficient, α_L , and the mixing time obtained for SBR 1500 loaded with 50 phr XLH142 (circles) and Sn-SSBR 1500 loaded with 50 phr XLH142 (squares).

Fig. 13 Relationship between the crosslinking density and the attenuation coefficient, α_L .

Fig. 14 Attenuation coefficient, α_L , as a function of temperature obtained for filled (50 phr N110 (circles), 50 phr XLH81 (squares)) and unfilled Sn-SSBR (triangles).

Fig. 15 Amplitude of the shear wave signal observed on the oscilloscope obtained as a function of temperature. The compound used was: Sn-SSBR loaded with 50 phr XLH81. The arrow marks the point on temperature scale where the attenuation coefficient, α_L , obtained for the longitudinal wave propagation has a maximum.

Fig. 16 Attenuation coefficient, α_T , obtained for the shear wave propagation as a function of temperature.

Fig. 17 Attenuation coefficient, α_L , obtained for different concentrations of loose N234 in ethyl alcohol.

Fig. 18 Master-curves obtained by applying the horizontal shift to measurements performed using a Rheometrics System IV Mechanical Spectrometer. The squares represent the data obtained for unfilled SBR1500, the triangles represent the data obtained for SBR 1500 filled with 50 phr N234 and the circles represent the difference between the two master-curves.

Fig. 19 The values of G' extrapolated to frequency 1 MHz and temperature 25°C using WLF equation.

Fig. 20 Attenuation coefficient, α_L , obtained for the same compounds as in Fig. 19.

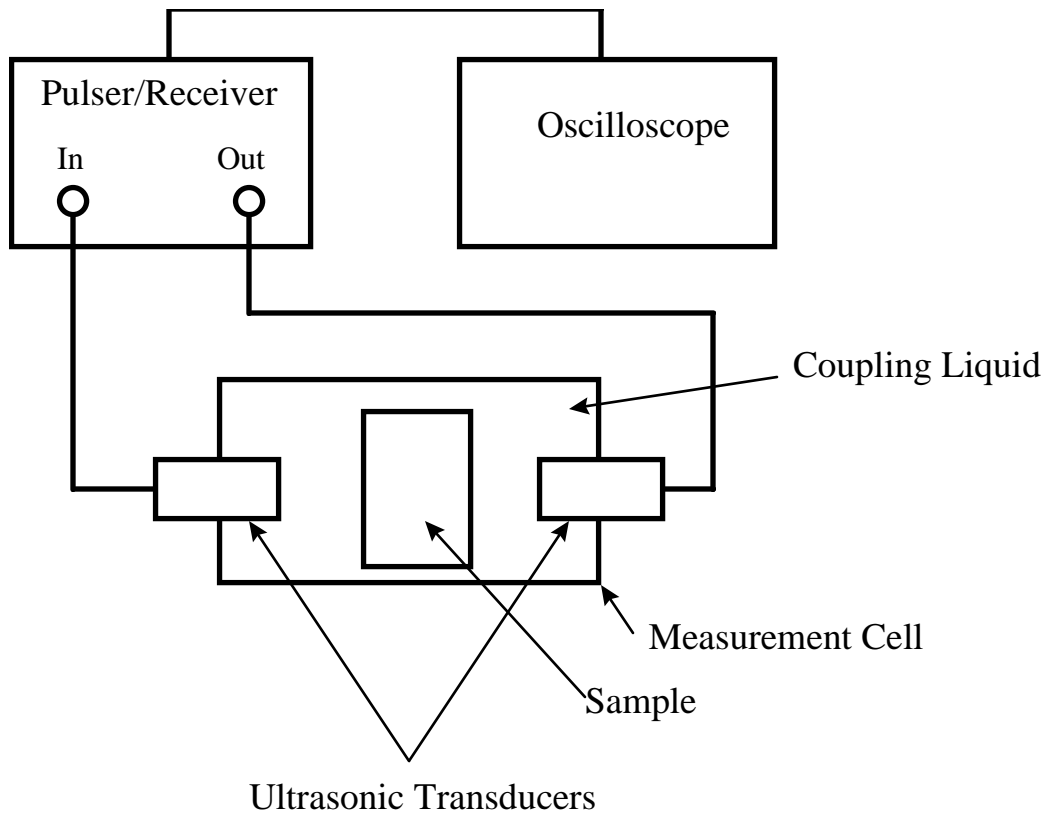


Fig. 1. M. Gerspacher *et al.* "High Frequency Viscoelasticity of Carbon Black Filled Compounds"

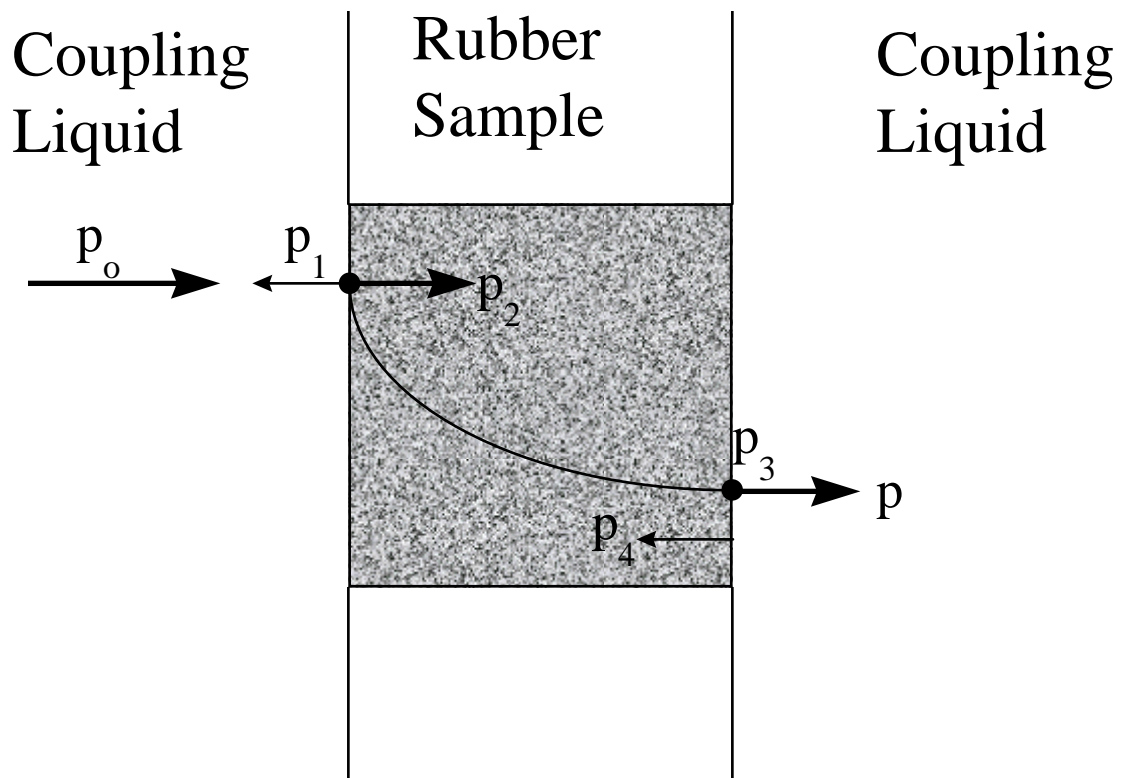


Fig. 2. M. Gerspacher *et al.* "High Frequency Viscoelasticity of Carbon Black Filled Compounds"

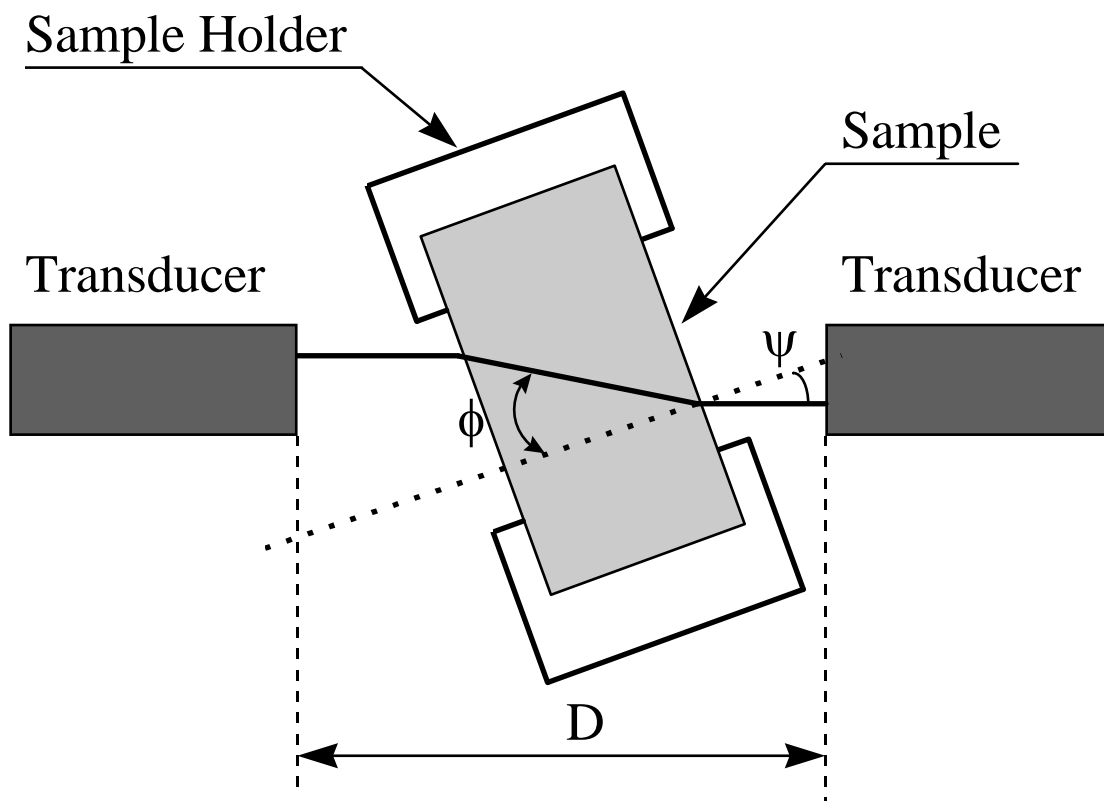


Fig. 3. M. Gerspacher *et al.* “High Frequency Viscoelasticity of Carbon Black Filled Compounds”

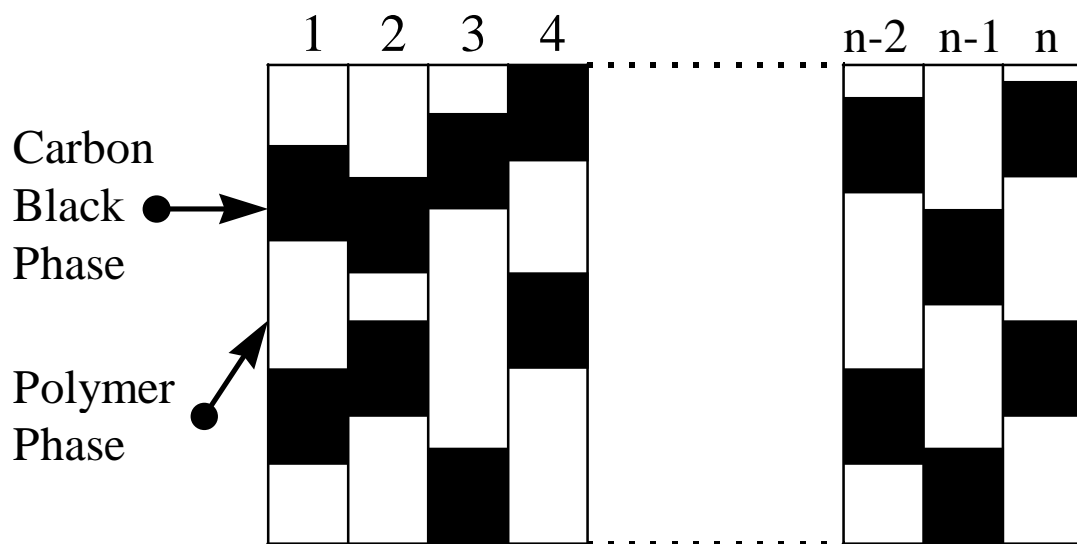


Fig. 4. M. Gerspacher *et al.* “High Frequency Viscoelasticity of Carbon Black Filled Compounds”

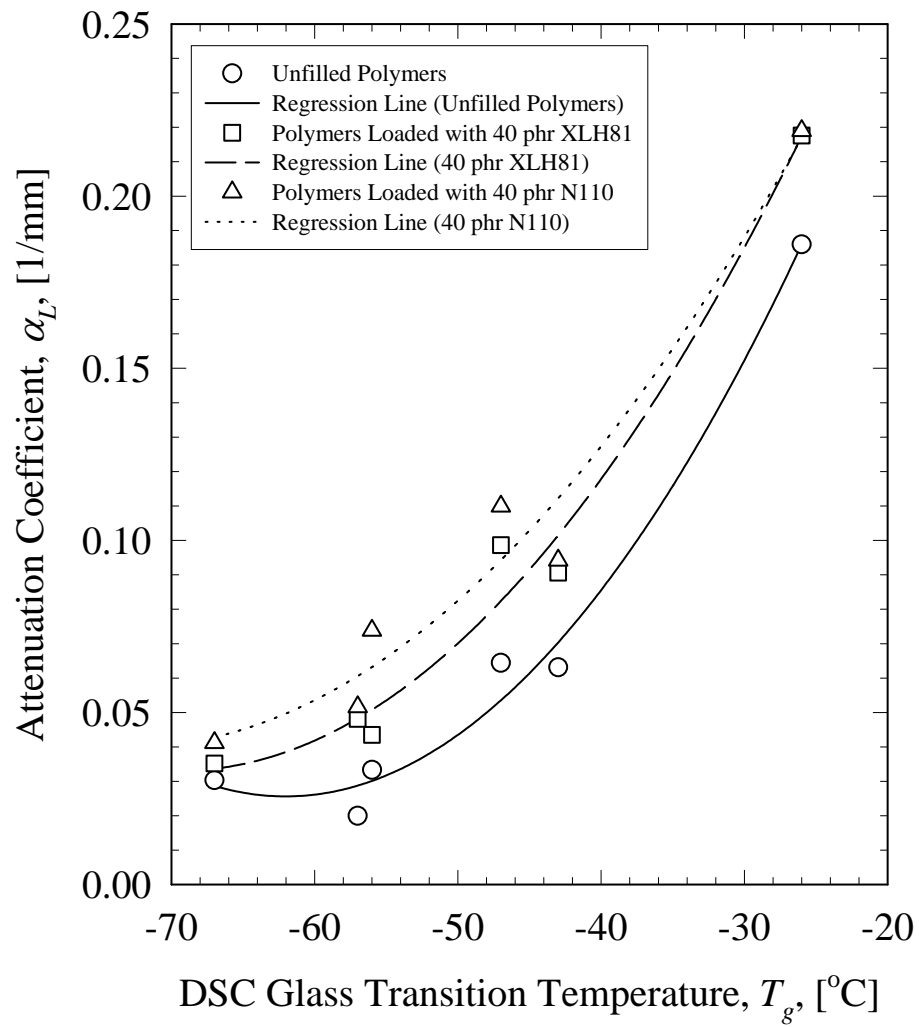


Fig. 5. M. Gerspacher *et al.* “High Frequency Viscoelasticity of Carbon Black Filled Compounds”

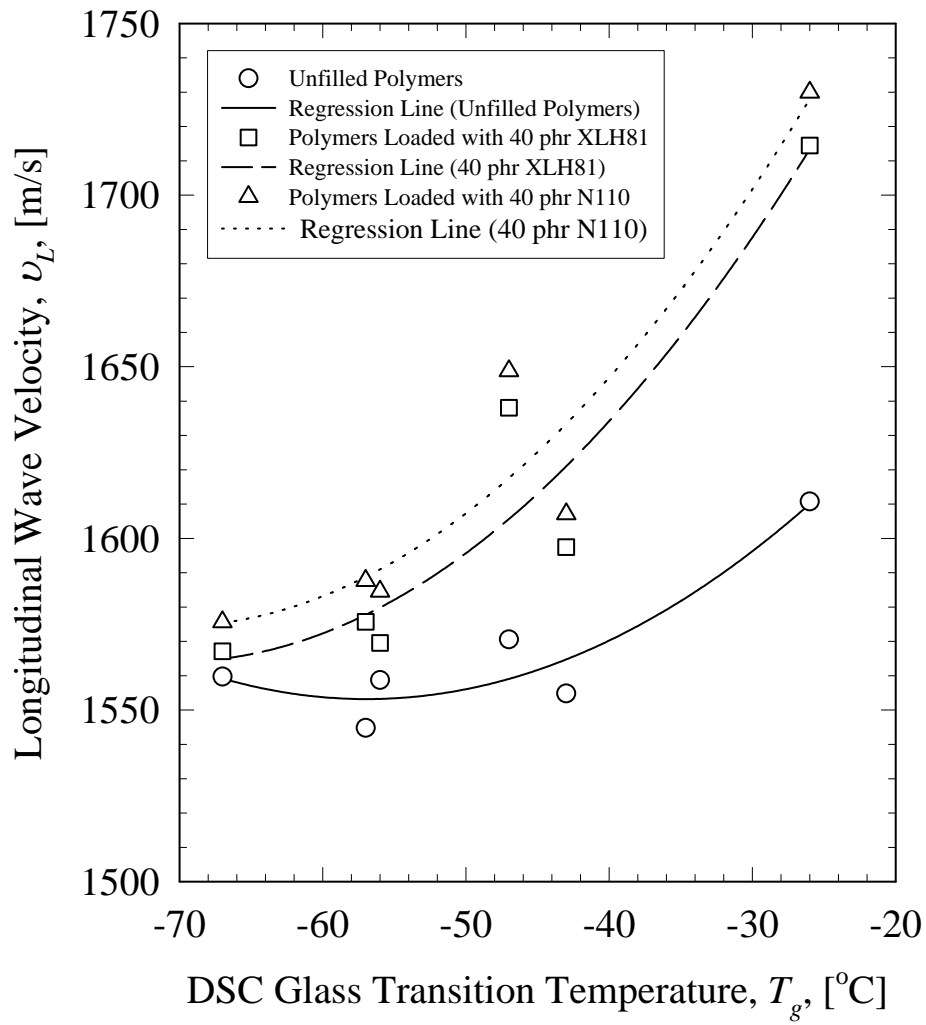


Fig. 6. M. Gerspacher *et al.* “High Frequency Viscoelasticity of Carbon Black Filled Compounds”

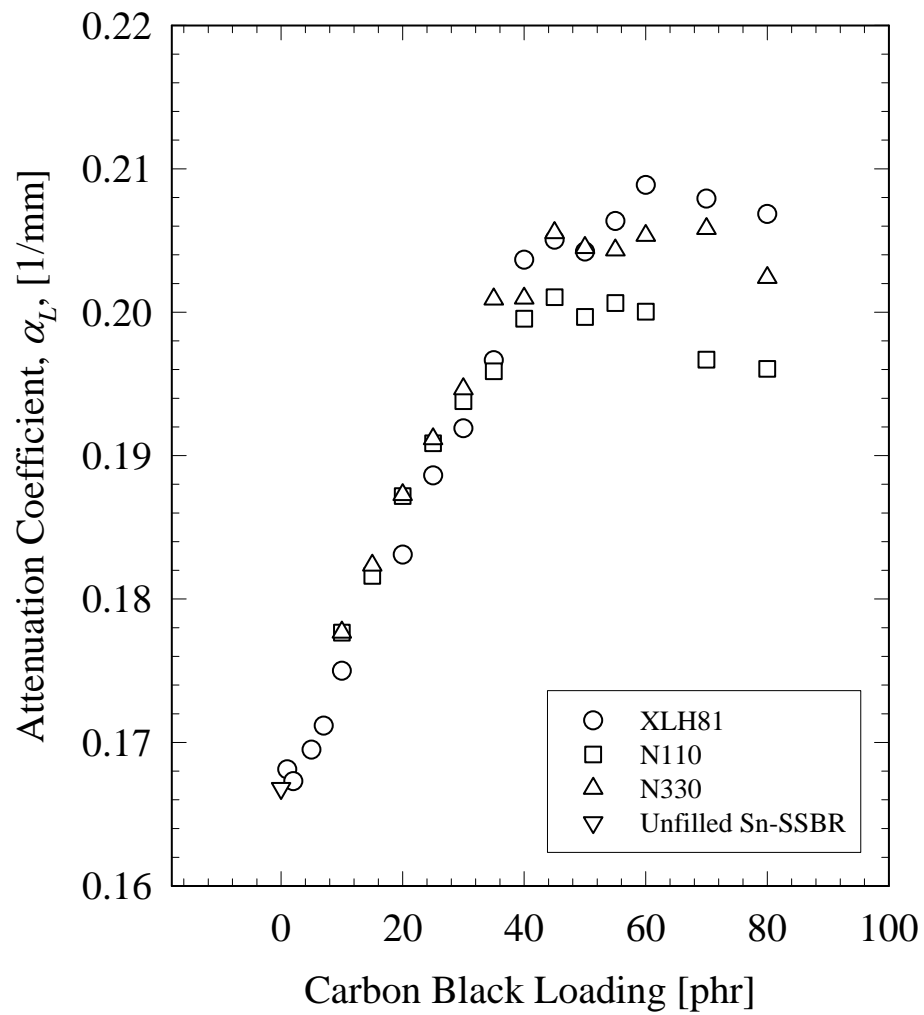


Fig. 7. M. Gerspacher *et al.* “High Frequency Viscoelasticity of Carbon Black Filled Compounds”

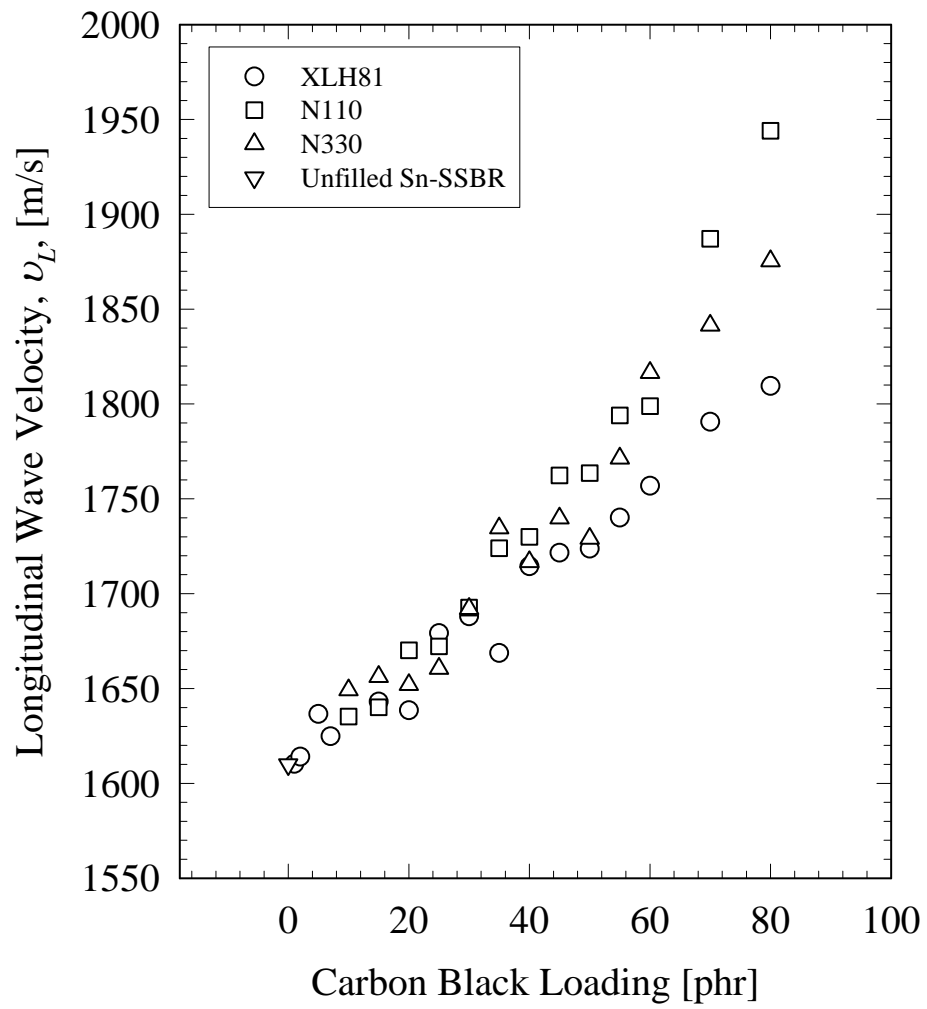


Fig. 8. M. Gerspacher *et al.* “High Frequency Viscoelasticity of Carbon Black Filled Compounds”

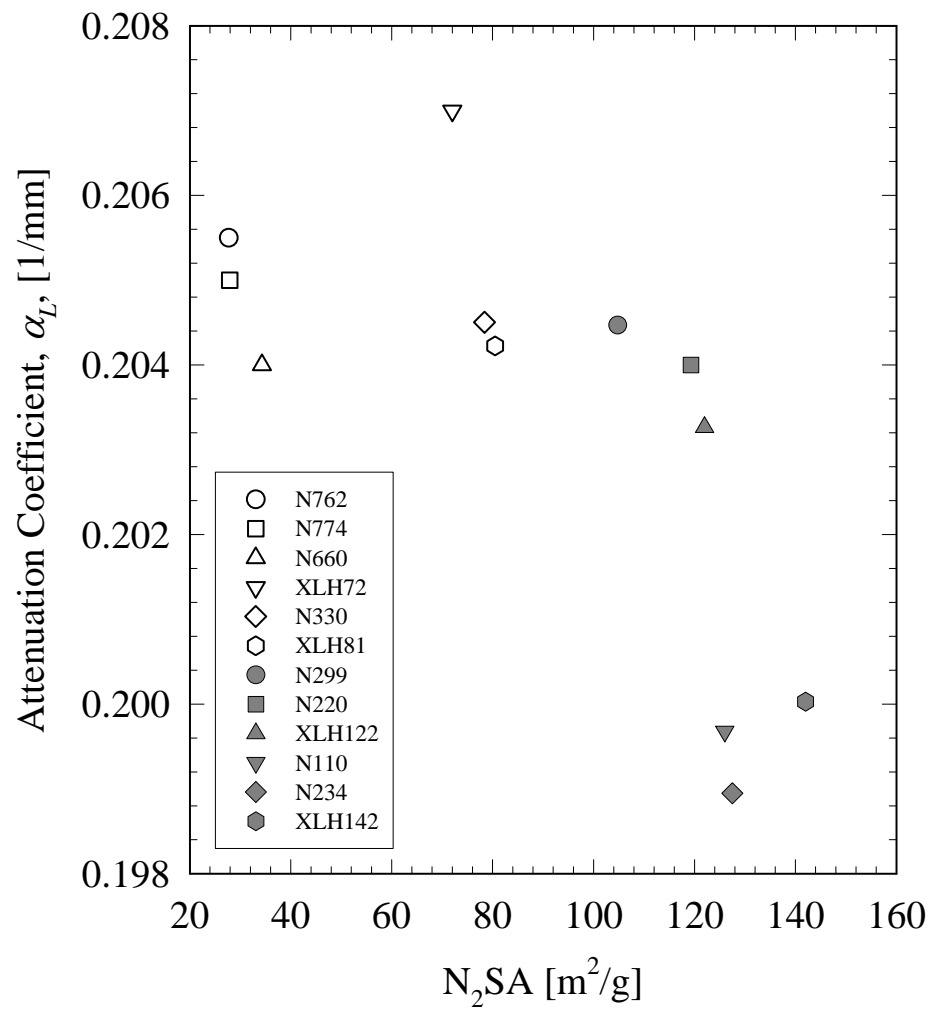


Fig. 9. M. Gerspacher *et al.* “High Frequency Viscoelasticity of Carbon Black Filled Compounds”

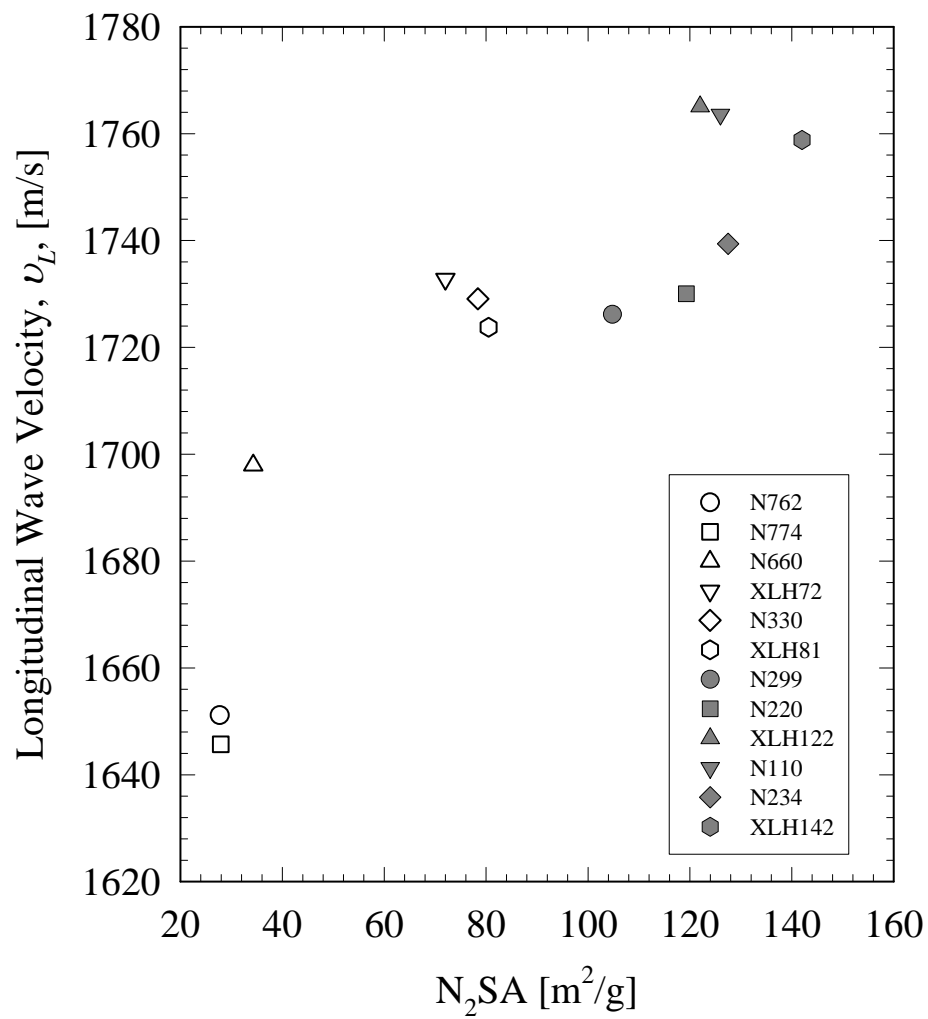


Fig. 10. M. Gerspacher *et al.* “High Frequency Viscoelasticity of Carbon Black Filled Compounds”

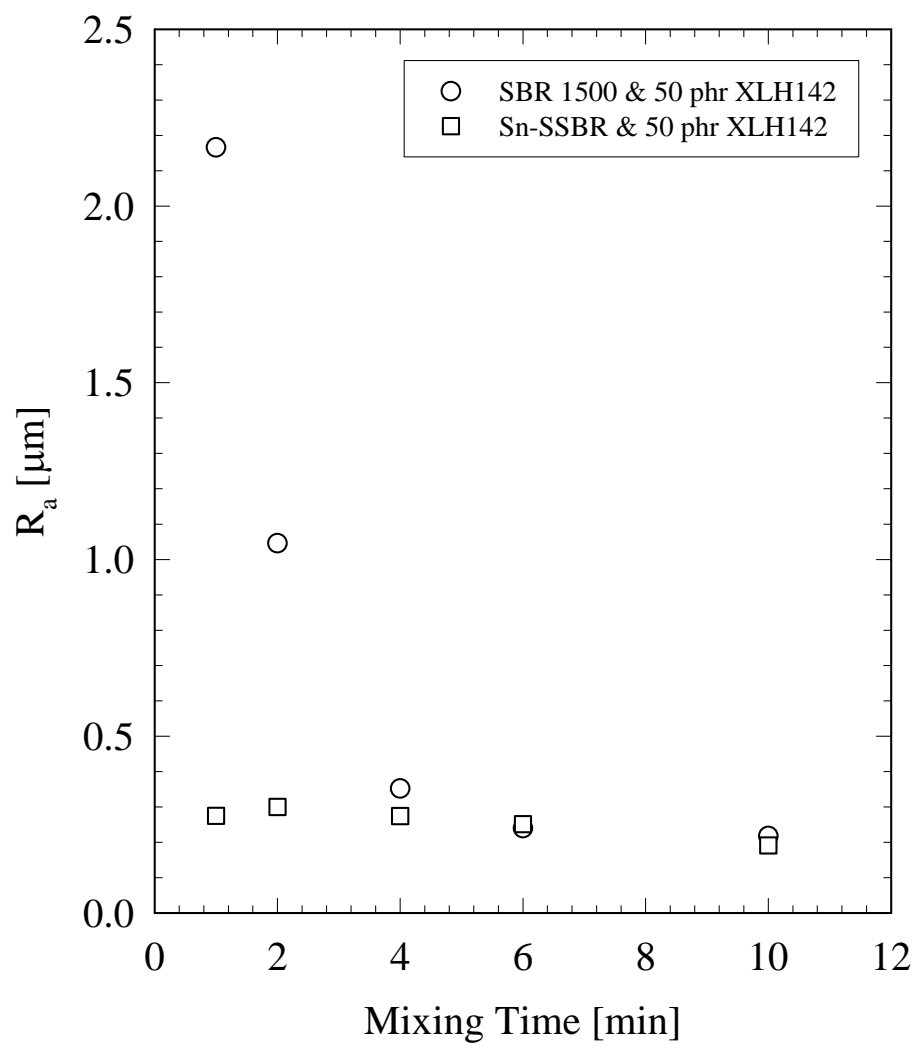


Fig. 11. M. Gerspacher *et al.* “High Frequency Viscoelasticity of Carbon Black Filled Compounds”

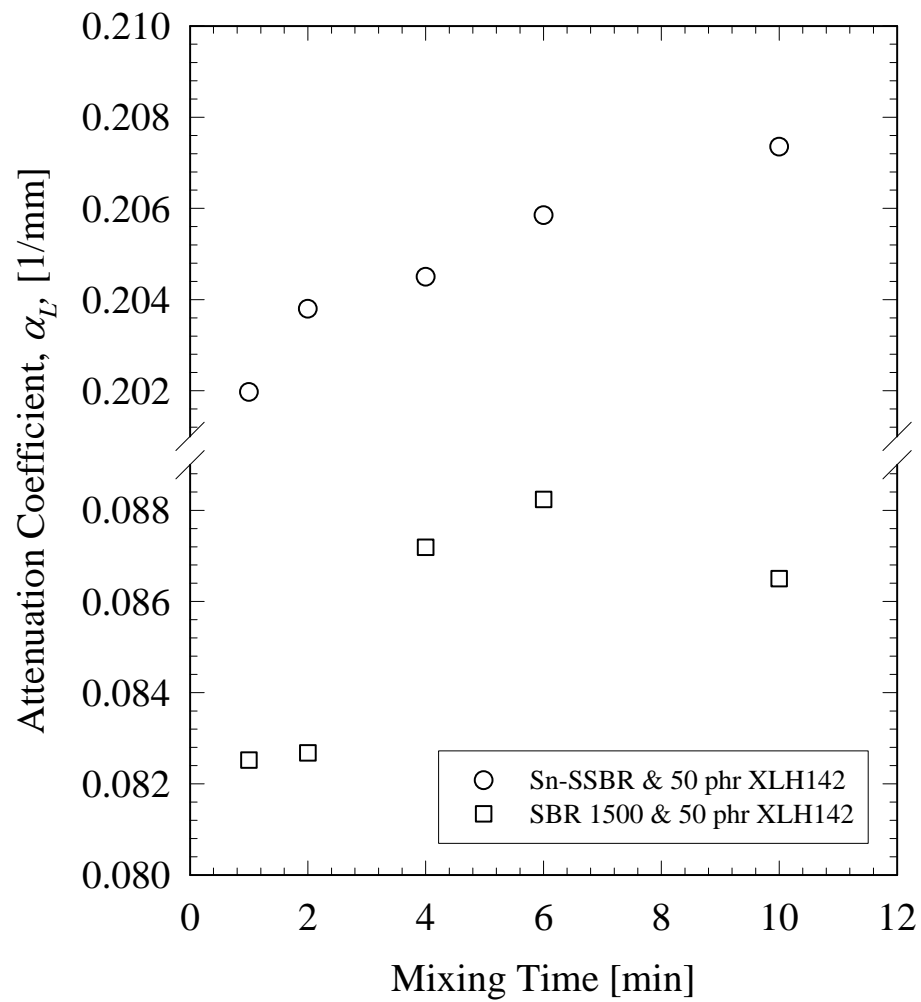


Fig. 12. M. Gerspacher *et al.* “High Frequency Viscoelasticity of Carbon Black Filled Compounds”

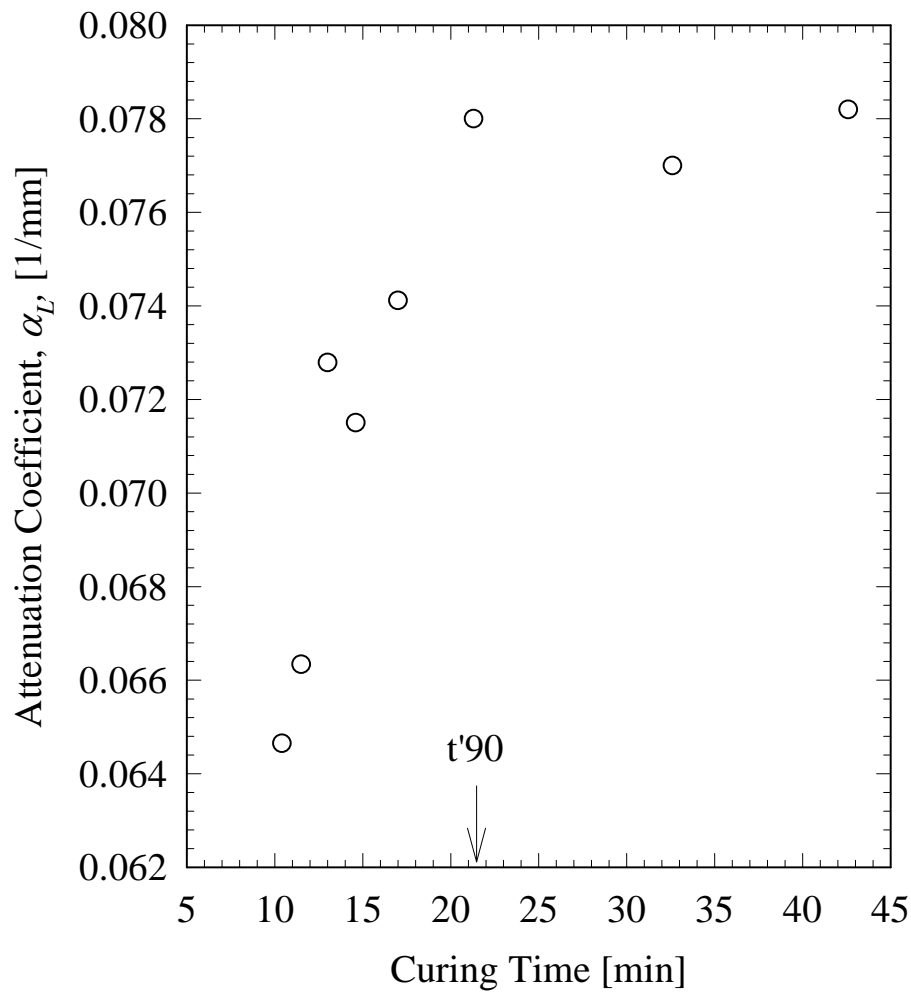


Fig. 13. M. Gerspacher *et al.* “High Frequency Viscoelasticity of Carbon Black Filled Compounds”

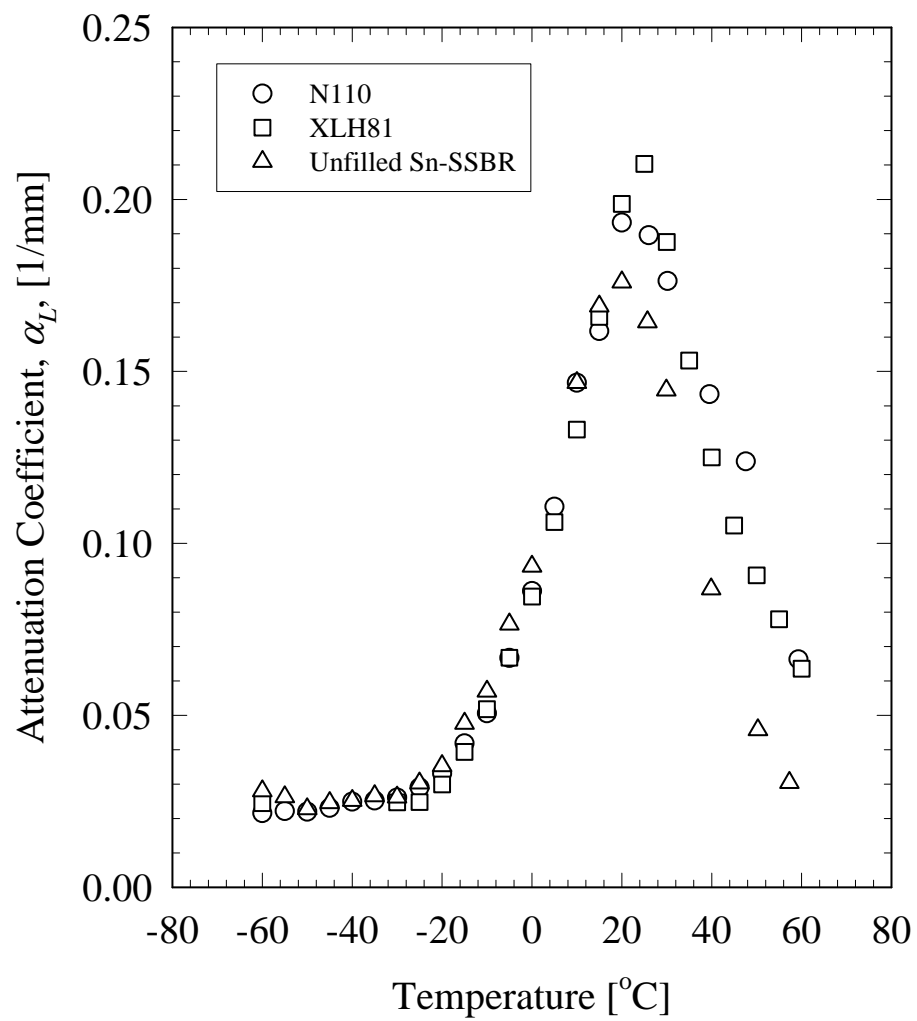


Fig. 14. M. Gerspacher *et al.* “High Frequency Viscoelasticity of Carbon Black Filled Compounds”

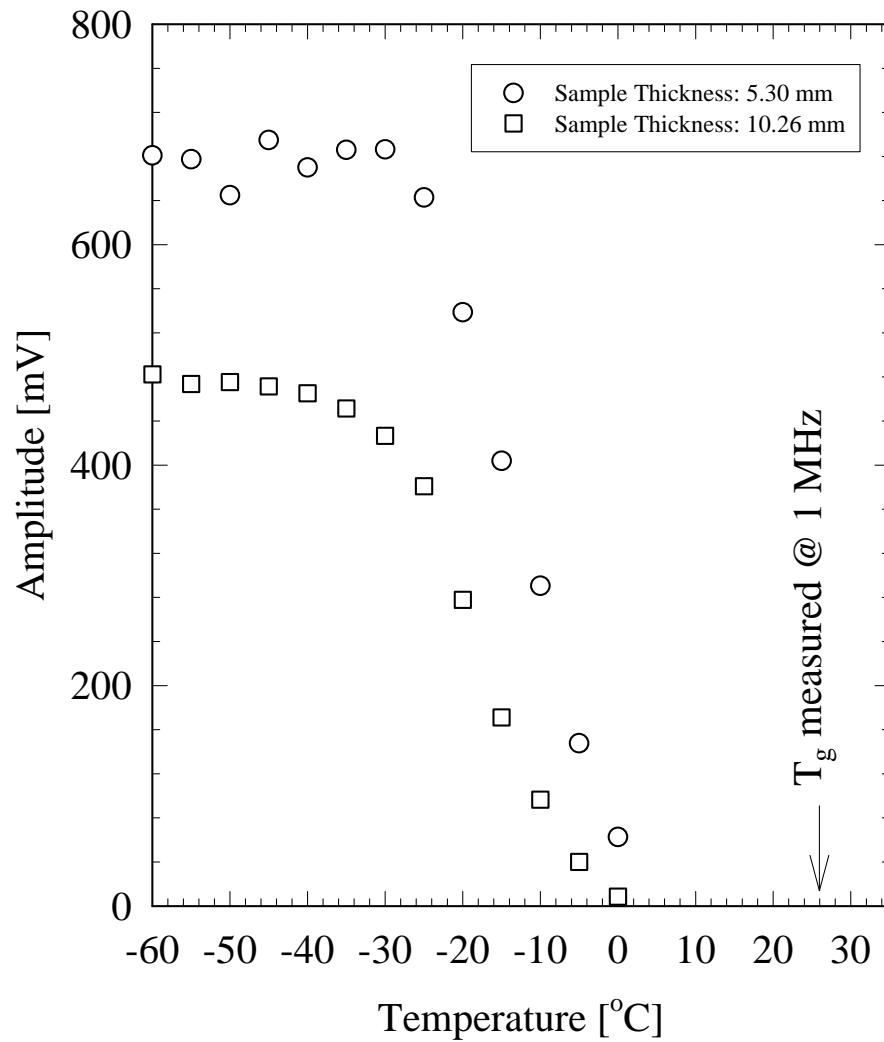


Fig. 15. M. Gerspacher *et al.* “High Frequency Viscoelasticity of Carbon Black Filled Compounds”

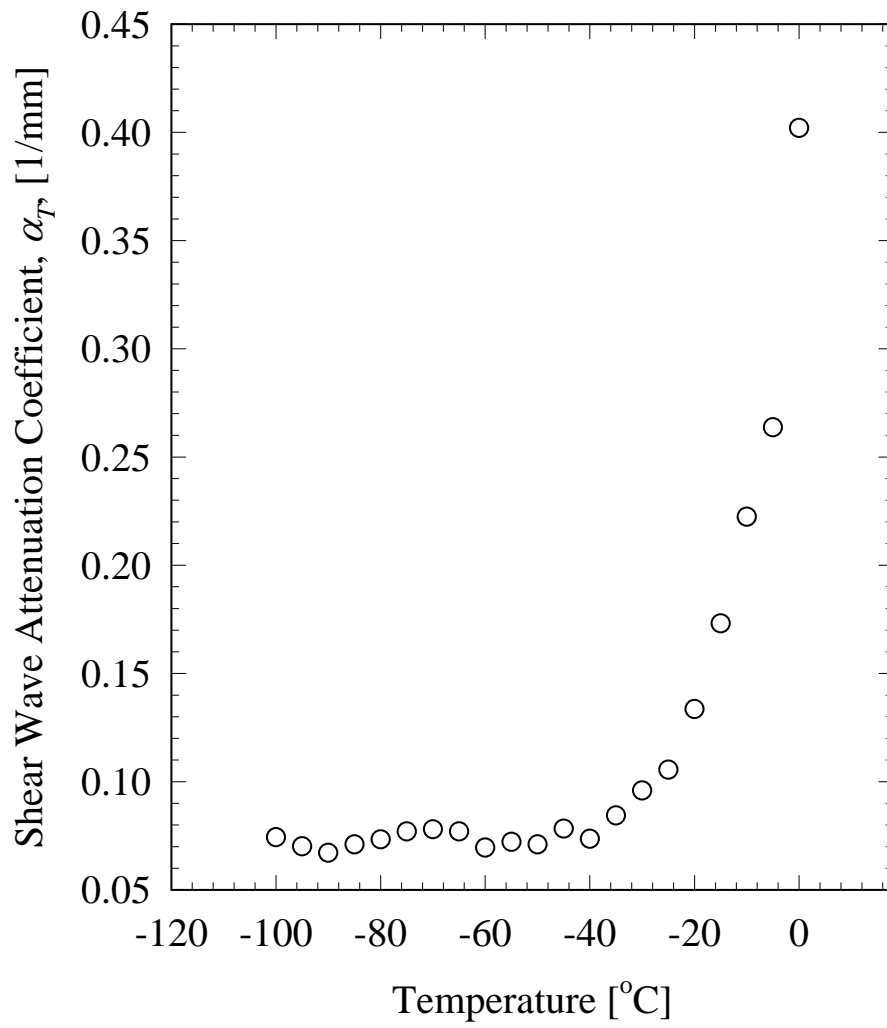


Fig. 16. M. Gerspacher *et al.* “High Frequency Viscoelasticity of Carbon Black Filled Compounds”

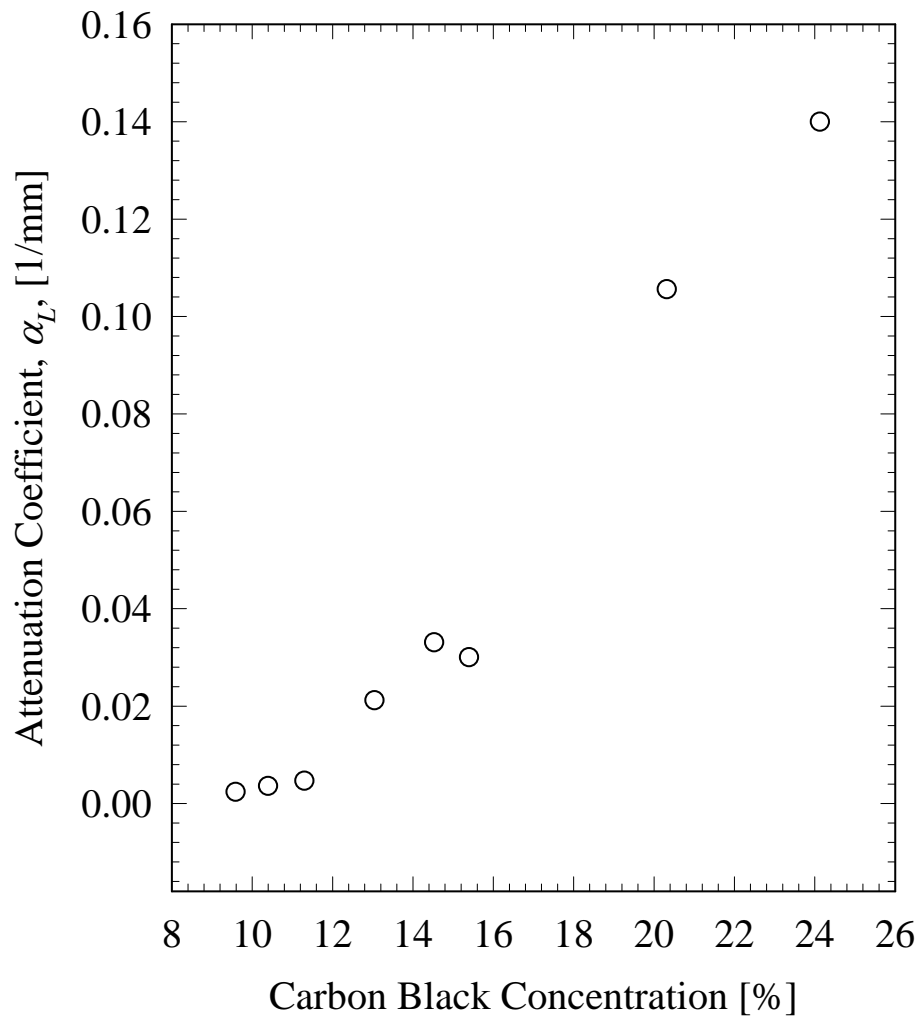


Fig. 17. M. Gerspacher *et al.* “High Frequency Viscoelasticity of Carbon Black Filled Compounds”

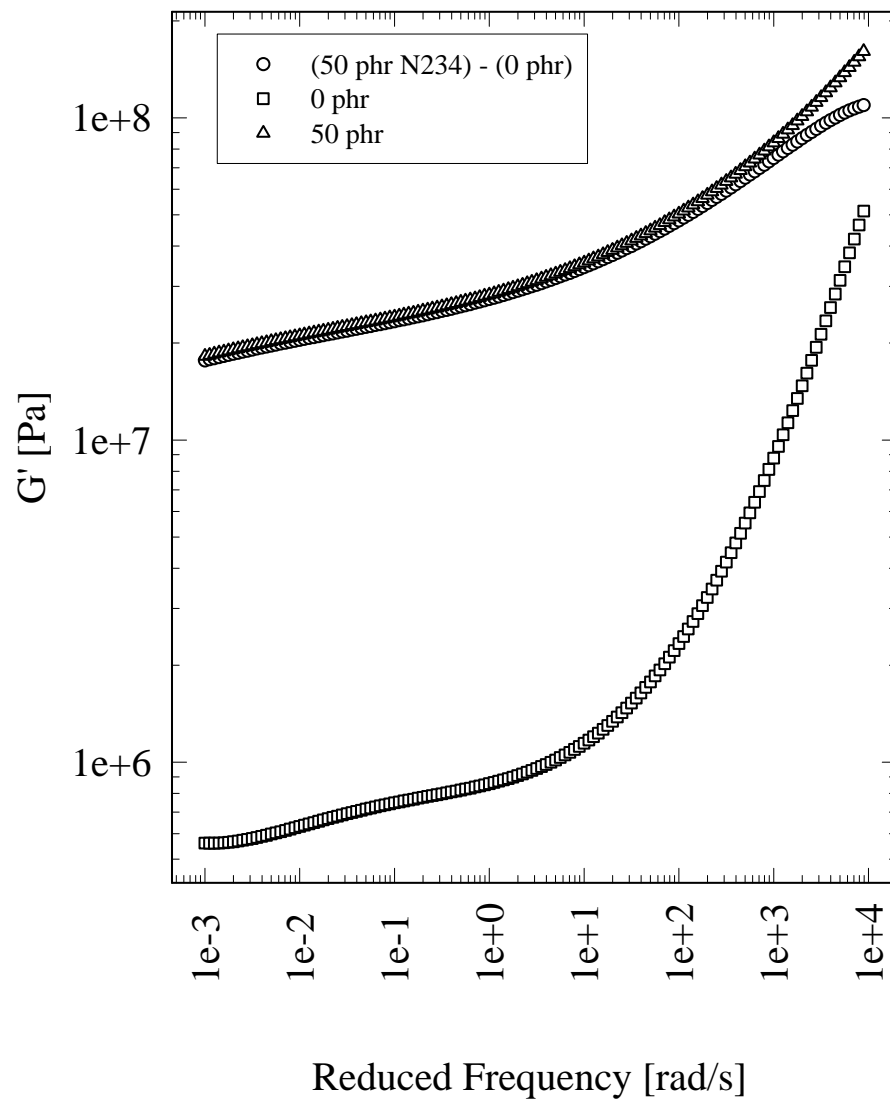


Fig. 18. M. Gerspacher *et al.* “High Frequency Viscoelasticity of Carbon Black Filled Compounds”

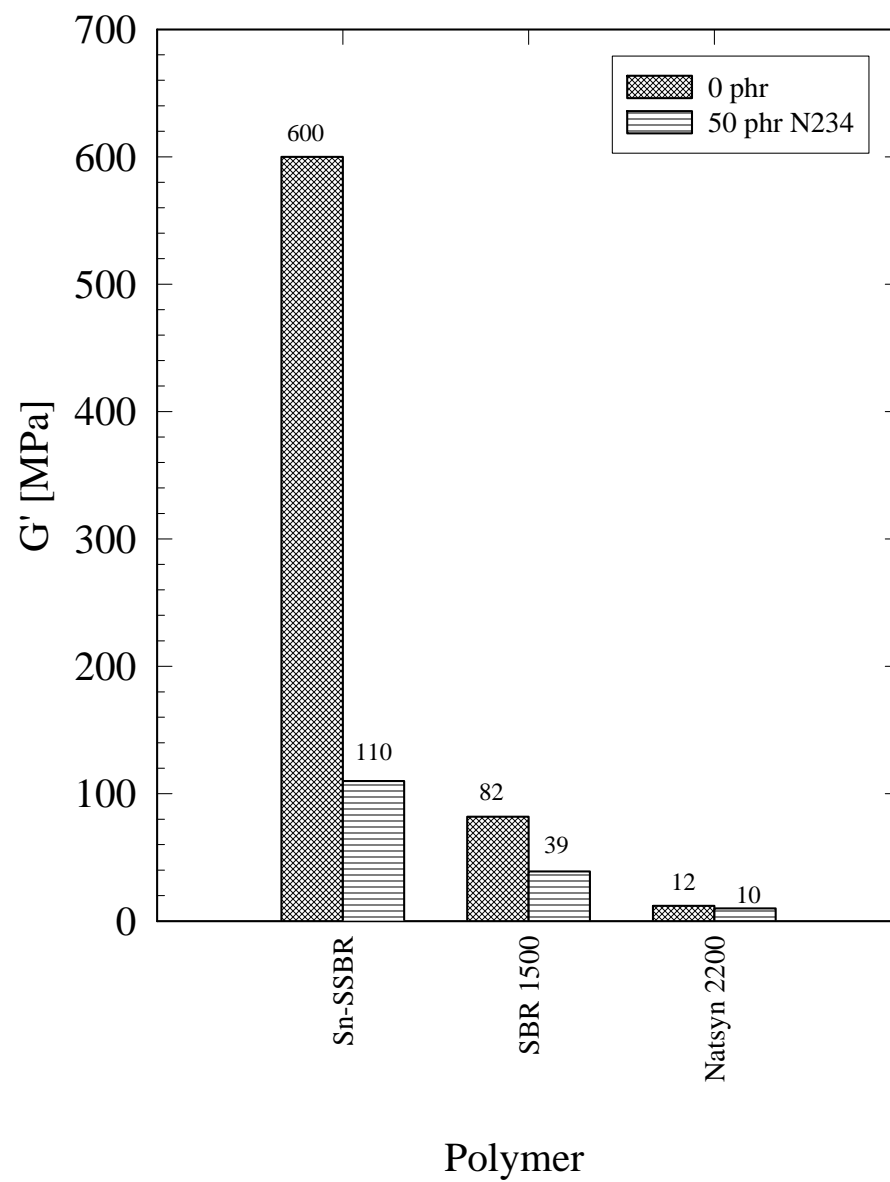


Fig. 19. M. Gerspacher *et al.* “High Frequency Viscoelasticity of Carbon Black Filled Compounds”

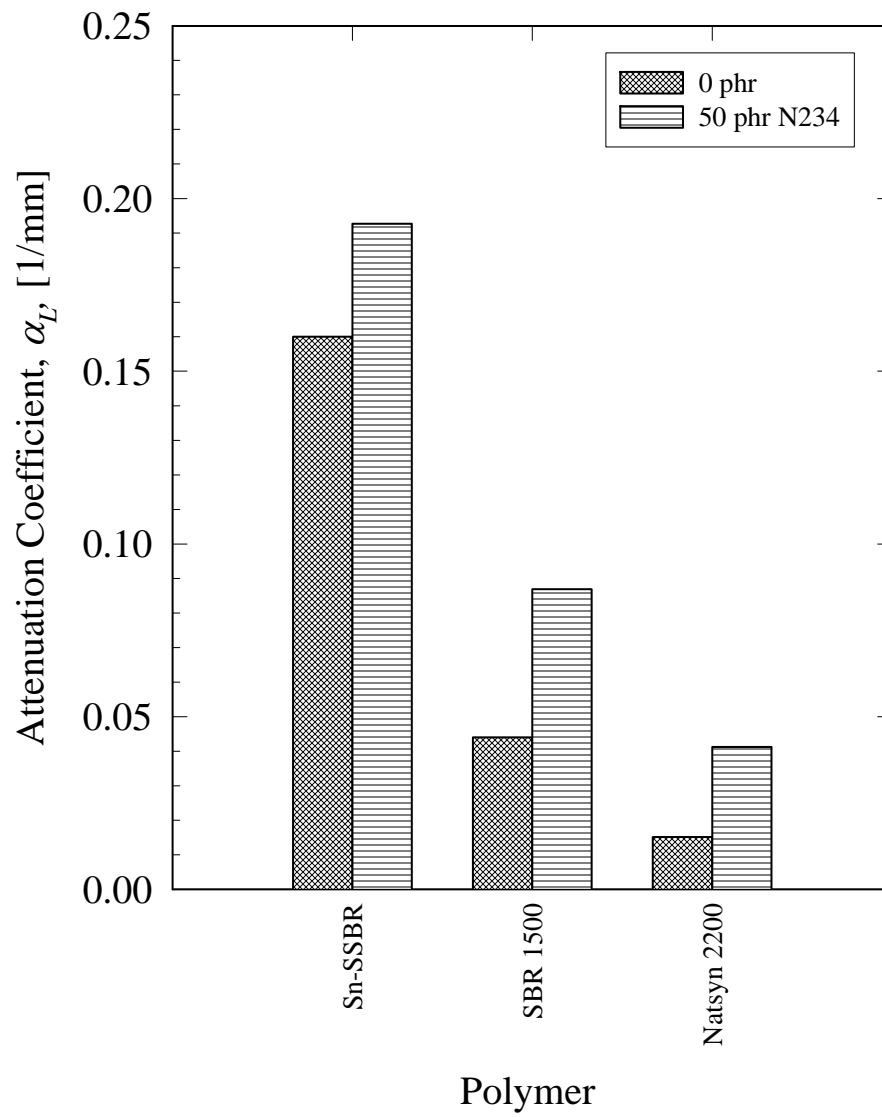


Fig. 20. M. Gerspacher *et al.* “High Frequency Viscoelasticity of Carbon Black Filled Compounds”

